JOURNAL OF THE AMERICAN CHEMICAL SOCIETY

COMMUNICATION

pubs.acs.org/JACS

Oxide Nanotubes on Ti–Ru Alloys: Strongly Enhanced and Stable Photoelectrochemical Activity for Water Splitting

Poulomi Roy,[†] Chittaranjan Das,[†] Kiyoung Lee,[†] Robert Hahn,[†] Tobias Ruff,[†] Matthias Moll,[‡] and Patrik Schmuki*[,†]

[†]Department of Materials Science, WW4-LKO, University of Erlangen-Nuremberg, Martensstrasse 7, D-91058 Erlangen, Germany

[‡]Department of Inorganic Chemistry, Universität Erlangen-Nürnberg, Egerlandstrasse 1, D-91058 Erlangen, Germany

Supporting Information

ABSTRACT: The present work shows a significant enhancement of the photoelectrochemical water-splitting performance of anodic TiO_2 nanotube layers grown on low concentration (0.01–0.2 at% Ru) Ti–Ru alloys. Under optimized preparation conditions (0.05 at% Ru, 450 °C annealing) the water splitting rate of the oxide tubes could be 6-fold increased. Moreover, the beneficial effect is very stable with illumination time; this is in contrast to other typical doping approaches of TiO_2.

Ever since Fujishima and Honda[1] reported on the photoelectrolysis of water into H_2 and O_2 on a TiO_2 electrode, much attention has been drawn to produce hydrogen from water or organic fuels using various photocatalyst materials under suitable light irradiation.[2–4] The water splitting reaction is based on the light induced electron–hole pair creation in a semiconductive material and the subsequent phase transfer reaction of the charge carriers to reduce/oxidize H_2O to H_2 and O_2. The main factors limiting the efficiency using pure TiO_2 as a water splitting photocatalyst are that (i) it can only absorb the UV light of the solar spectrum (owing to the wide band gap of 3.0–3.2 eV) and that (ii) only a sluggish charge transfer kinetics to H_2O is obtained. Main efforts are therefore directed to enhance the photocatalytic material by band gap engineering (narrowing the band gap and aligning the band-edge positions) and to facilitate charge transfer by maximizing the surface area and using charge-transfer catalysts.[5–11] In terms of band gap engineering to narrow the band gap, most widely used are nitrides or oxonitrides.[12,13] However, these materials tend to photodecompose, and thus they typically lack a sufficient long-term stability.[12] In contrast, TiO_2 is photostable, but to achieve reasonably efficient H_2 evolution, the electron transfer reaction to the electrolyte needs to be catalyzed, typically using either Pt nanoparticles[14–16] or a photoelectrochemical arrangement, where the TiO_2 based photocatalyst is used as a photoanode in combination with a separate Pt cathode. Additionally, for catalyzing the O_2 production reaction, some work used TiO_2 decorated with RuO_2 nanoparticles, this with variable success.[17–19] In order to achieve a reasonable overall efficiency, high surface area photoanodes are required that are built of a nanoscale TiO_2 network, for example by fabricating layers of compacted nanoparticles.

Most recently, a highly promising route to obtain efficient and highly defined nanoscale photoelectrodes has been reported, which is the anodic growth of self-organized TiO_2 nanotube layers on Ti. Length, diameter, and crystallinity of such layers can be adjusted by the selection of the anodization parameters[20] and the thermal post-treatment.[21] These TiO_2 nanotubular layers grow vertically aligned on the Ti substrate (i.e., represent directly back contacted electrodes) and were reported to show excellent photoelectrochemical properties, which are significantly enhanced compared with nanoparticulate layers.[5,22,23]

In the present work, we demonstrate how a strong improvement of the water splitting activity of such nanotubular anodes can be achieved if the oxide nanotubes are grown by anodizing a Ti–Ru alloy substrate under self-organizing oxide-tube forming conditions. The resulting nanotube oxide layers, after an appropriate heat treatment, not only show strongly enhanced water splitting ability, in comparison to an undoped TiO_2 nanotube sample, but also provide (in contrast to many other doping attempts[12]) long-term stability. Moreover, this approach, where an alloy is used to grow oxide tubes, is found to be much more efficient than any attempt to achieve a similar effect by decorating pure TiO_2 nanotubes with RuO_2 nanoparticles.

An example of a Ru-doped TiO_2 nanotube layer is shown in the SEM images of Figure 1a,b. The 4 μm thick layer was grown on a 0.05 at% Ti–Ru alloy by electrochemical anodization in an ethylene glycol electrolyte containing 0.2 M HF (experimental details on alloy preparation and anodization are given in the Supporting Information (SI)). Self-organized oxide nanotubes were grown on substrates with different amounts of Ru (containing 0.01 at%, 0.05 at%, 0.1 at%, 0.2 at%, 0.5 at%, and 1.2 at%). SEM images are given in the SI (Figure S1). For Ru concentrations higher than 1.2 at%, anodization resulted in increasingly disordered nanotube layers, and at concentrations >5 at% only highly random porous oxide layers were obtained. For all the samples it was found that the as-grown nanotube layers are amorphous as shown in the SAED pattern in Figure 1c–d and the XRD spectra in Figure 1f (shown for the 0.05 at% Ru sample). To crystallize the tubes, we annealed the samples at various temperatures. Figure 1e shows the SAED pattern, and Figure 1f the XRD pattern after annealing the 0.05 at% sample at 450 °C. Both XRD and SAED patterns show the conversion to anatase with a small amount of rutile. Although crystallization of RuO_2 is expected to take place around 300 °C,[24] in the XRD pattern, this conversion could not be observed due to the low Ru concentration. The presence of RuO_2 can, however, be

Received: December 8, 2010
Published: March 29, 2011

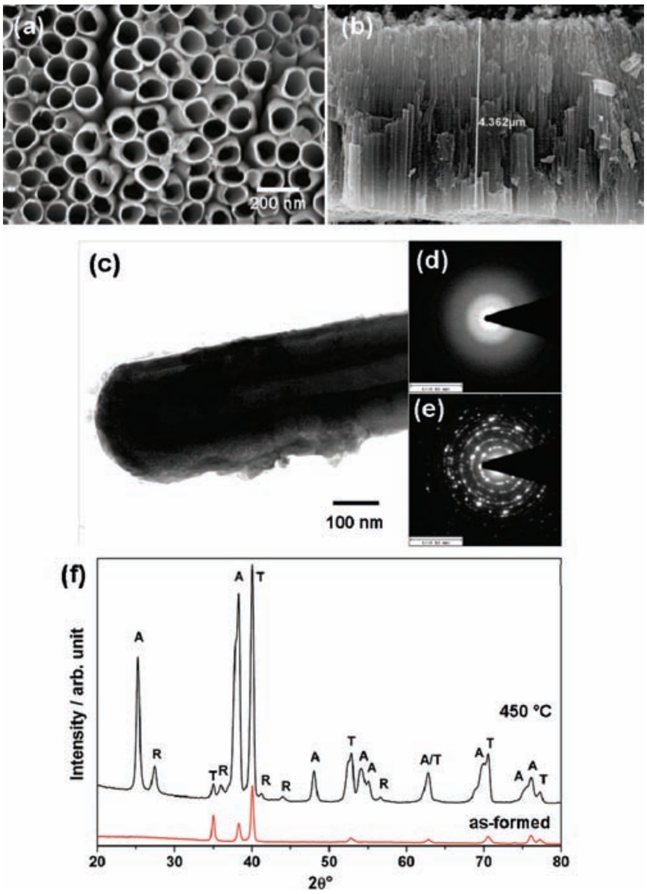

Figure 1. (a) Top view and (b) cross-sectional view SEM images of 0.05 at% Ru doped TiO_2 nanotube layers. (c) TEM image of an as-grown single nanotube doped with 0.2 at% Ru and the corresponding SAED pattern (d) before and (e) after annealing. (f) XRD pattern of 0.05 at% Ru doped TiO_2 nanotube layers, as-formed and after annealing at 450 °C for 1 h, revealing mostly anatase TiO_2 and no significant RuO_2 peak due to a very low doping concentration (A, anatase; R, rutile; T, titanium).

confirmed by the TOF-SIMS analysis (see SI, Figure S2). This uptake, however, does not change the optical absorption characteristics significantly (Figure S3). For different annealing temperatures, the amount of rutile phase increases, and at 650 °C, the nanotube layer transformed mostly into a rutile phase and a minor amount of anatase (see SI, Figure S4).

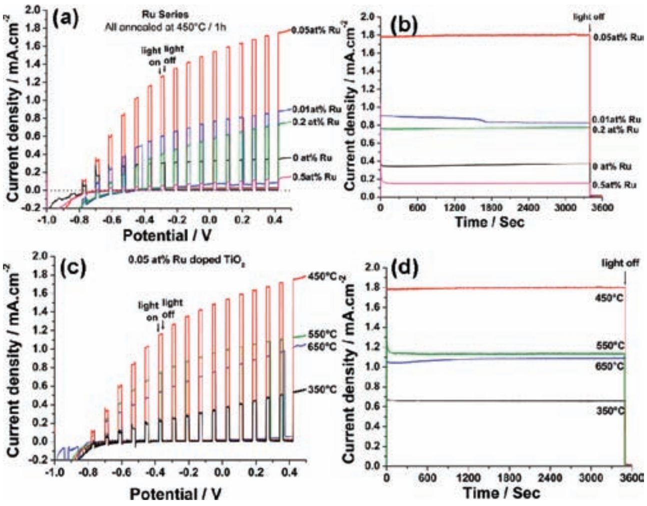

Figure 2. (a) Photocurrent transient vs potential curves of different Ru substrate contents (0−1.2 at%) TiO_2 nanotube layers after annealing at 450 °C for 1 h and (b) corresponding photostability experiment for 1 h holding at 500 mV. (c) Photocurrent transient vs potential curves for 0.05 at% Ru content layers after annealing at different temperatures (350−650 °C) and (d) photostability experiment holding at 500 mV. All experiments were carried out in 1 M KOH solution using a Ag/AgCl reference electrode under AM 1.5 illumination.

Figure 2 shows an assessment of different tubes in terms of their photoelectrochemical water splitting performance under simulated sunlight AM 1.5 conditions. From the photocurrent transient vs potential curves, it is apparent that the nanotubes grown on Ru alloys can show a significantly enhanced performance in comparison with undoped TiO_2 nanotubes. If the tubes are annealed at various temperatures a maximum efficiency can be found for 450 °C (Figure 2c−d). It is also evident that an optimum concentration of 0.05 at% Ru exists. These tubes, after annealing at 450 °C, show an almost 6-fold increase of the photocurrent compared with nondoped TiO_2 nanotubes. Accordingly, GC analysis revealed a H_2 production rate of 45 μmol/h/cm^2 (measured at 500 mV), which indicates a nearly 100% conversion of the current to H_2 with an H_2/O_2 ratio of ~2:1. For all nanotube layers an increase in the photocurrent with an increase in the applied potential can be observed with a dark current that remains very low (<5 μA). If the photoelectrochemical water splitting efficiency is evaluated (as shown in the SI, Figure S6), an increase from 0.25% for pure TiO_2 nanotubes to 0.91% for the nanotube layers on the alloy is obtained. A very important finding is that the Ru effect is extremely stable (Figure 2b); i.e., the beneficial effect does not deteriorate with time. Even if the experiment is carried out for 14 h, no significant drop in the photocurrent (H_2 production rate) can be observed (see SI, Figure S7). This is a key advantage over other doping approaches, using N- or C-doping in TiO_2 or Ta_2O_5, where a significant drop in efficiency is reported with illumination time (for example, the water splitting efficiency of TaON drops by 80% within 5 min under similar illumination conditions[12]). Moreover, it should be pointed out that the present approach is far superior to attempts that apply the RuO_2 catalyst to the TiO_2 nanotubes by nanoparticle loading. This is shown in the SI (Figure S8) where TiO_2 nanotubes were decorated with RuO_2 nanoparticles using various procedures,[25] where the water splitting performance could only mildly be influenced by particle decoration; i.e., the bulk-doping process introduced in the present paper yields a significantly higher performance.

In conclusion, we demonstrate a strong and stable enhancement of the photoelectrochemical water splitting activity of anodic TiO_2 nanoube layers grown by anodization on low concentration Ru in Ti−Ru alloys. The effect is far superior to attempts using RuO_2 nanoparticles as a surface catalyst. The overall water splitting efficiency depends on the Ru content and the annealing conditions. Under an optimized preparation procedure the water splitting rate of TiO_2 nanotubes could be almost 6-fold increased in comparison with undoped TiO_2 nanotube layers.

■ ASSOCIATED CONTENT

Ⓢ Supporting Information. Experimental details, SEM images, TOF-SIMS analysis, XRD analysis, photoelectrochemical measurements of the samples. This material is available free of charge via the Internet at http://pubs.acs.org.

AUTHOR INFORMATION

Corresponding Author
schmuki@ww.uni-erlangen.de

ACKNOWLEDGMENT

The authors are thankful to Mrs. Helga Hilderbrand for TOF-SIMS analysis and acknowledge financial support from the DFG and the DFG Cluster of Excellence (EAM).

REFERENCES

(1) Fujishima, A.; Honda, K. *Nature* **1972**, *238*, 37.

(2) (a) Bard, A. J. *Science* **1980**, *207*, 139–144. (b) Fujishima, A.; Zhang, X.; Tryk, D. A. *Surf. Sci. Rep.* **2008**, *63*, 515–582. (c) Maeda, K.; Domen, K. *J. Phys. Chem. Lett.* **2010**, *1*, 2655–2661.

(3) (a) Borgarello, E.; Kivi, J.; Pelizzetti, E.; Visca, M.; Grätzel, M. *Nature* **1981**, *289*, 158–160. (b) Grätzel, M. *Acc. Chem. Res.* **1981**, *14*, 376–384.

(4) (a) Kudo, A. *Catal. Surv. Asia* **2003**, *7*, 31–38. (b) Kudo, A. *Pure Appl. Chem.* **2007**, *79*, 1917–1924. (c) Niishiro, R.; Kato, H.; Kudo, A. *Phys. Chem. Chem. Phys.* **2005**, *7*, 2241–2245.

(5) Park, J. H.; Kim, S.; Bard, A. J. *Nano Lett.* **2006**, *6*, 24–28.

(6) Zuo, F.; Wang, L.; Wu, T.; Zhang, Z.; Borchardt, D.; Feng, P. *J. Am. Chem. Soc.* **2010**, *132*, 11856–11857.

(7) Shevlin, S. A.; Woodley, S. M. *J. Phys. Chem. C* **2010**, *114*, 17333–17343.

(8) Yin, W.-J.; Tang, H.; Wei, S.-H.; Al-Jassim, M. M.; Turner, J.; Yan, Y. *Phys. Rev. B* **2010**, *82*, 045106.

(9) Palmas, S.; Polcaro, A. M.; Ruiz, J. R.; Da Pozzo, A.; Mascia, M.; Vacca, A. *Int. J. Hydrogen Energy* **2010**, *35*, 6561–6570.

(10) Khan, S. U. M.; Al-Shahry, M.; Ingler, W. B., Jr. *Science* **2002**, *297*, 2243–2245.

(11) Sato, S. *Chem. Phys. Lett.* **1986**, *123*, 126–128.

(12) Abe, R.; Higashi, M.; Domen, K. *J. Am. Chem. Soc.* **2010**, *132*, 11828–11829.

(13) Banerjee, S.; Mohapatra, S. K.; Misra, M. *Chem. Commun.* **2009**, 7137–7139.

(14) Kandiel, T. A.; Dillert, R.; Robben, L.; Bahnemann, D. W. *Catal. Today* **2011**, *161*, 196–201.

(15) Yu, J.; Qi, L.; Jaroniec, M. *J. Phys. Chem. C* **2010**, *114*, 13118–13125.

(16) Galińska, A.; Walendziewski, J. *Energy Fuels* **2005**, *19*, 1143–1147.

(17) Kawai, T.; Sakata, T. *Nature* **1980**, *286*, 474.

(18) Blondeel, G.; Harrlman, A.; Porter, G.; Urwln, D.; Kiwi, J. *J. Phys. Chem.* **1983**, *87*, 2629–2636.

(19) Sakata, T.; Hashimoto, K.; Hawai, T. *J. Phys. Chem.* **1984**, *88*, 5214–5221.

(20) (a) Roy, P.; Berger, S.; Schmuki, P. *Angew. Chem. Int. Ed.* **2010**, *50*, 2904–2939. (b) Ghicov, A.; Schmuki, P. *Chem. Commun.* **2009**, 2791–2808.

(21) Albu, S. P.; Ghicov, A.; Aldabergenova, S.; Drechsel, P.; LeClere, D.; Thompson, G. E.; Macak, J. M.; Schmuki, P. *Adv. Mater.* **2008**, *20*, 4135–4139.

(22) (a) Macak, J. M.; Zlamal, M.; Krysa, J.; Schmuki, P. *Small* **2007**, *3*, 300–304.(b) Das, C.; Roy, P.; Yang, M.; Schmuki, P. In preparation.

(23) Allam, N. K.; Shankar, K.; Grimes, C. A. *J. Mater. Chem.* **2008**, *18*, 2341–2348.

(24) Bhaskar, S.; Majumder, S. B.; Dobal, P. S.; Katiyar, R. S.; Cruz, A. L. M.; Fachini, E. R. In Chemical Processing of Dielectrics, Insulators and Electronic Ceramics; Jones, A. C., Veteran, J., Kaushal, S., Mullin, D., Cooper, R., Eds. (*Mater. Res. Soc. Symp. Proc.* **2000**, *606*, Warrendale, PA), 218922.

(25) Amama, P. B.; Itoh, K.; Murabayashi, M. *J. Mater. Sci.* **2004**, *39*, 4349–4351.